

This is an Open Access document downloaded from ORCA, Cardiff University's institutional repository: <https://orca.cardiff.ac.uk/id/eprint/150278/>

This is the author's version of a work that was submitted to / accepted for publication.

Citation for final published version:

Borodich, F.M , Galanov, B.A and Grigoriev, O.N 2022. Adhesion and wear of diamond: Formation of nanocracks and adhesive craters of torn out material. Philosophical Transactions of the Royal Society A: Mathematical, Physical and Engineering Sciences 10.1098/rsta.2021.0341

Publishers page: <https://doi.org/10.1098/rsta.2021.0341>

Please note:

Changes made as a result of publishing processes such as copy-editing, formatting and page numbers may not be reflected in this version. For the definitive version of this publication, please refer to the published source. You are advised to consult the publisher's version if you wish to cite this paper.

This version is being made available in accordance with publisher policies. See <http://orca.cf.ac.uk/policies.html> for usage policies. Copyright and moral rights for publications made available in ORCA are retained by the copyright holders.





Article submitted to journal

Subject Areas:

Solid Mechanics, Contact Mechanics,
xxxxx

Keywords:

diamond, nanocracks, adhesive
contact, JKR theory, abrasive wear

Author for correspondence:

Feodor M. Borodich
e-mail: BorodichFM@cardiff.ac.uk

Adhesion and wear of diamond: Formation of nanocracks and adhesive craters of torn out material

Feodor M. Borodich^{1,2}, Boris A. Galanov³,
and Oleg N. Grigoriev³

¹ College of Aerospace Engineering, Chongqing
University, Chongqing, China, ² School of Engineering,
Cardiff University, Cardiff, UK,

³ Institute for Problems in Materials Science, National
Academy of Sciences of Ukraine, Kiev, Ukraine

Mechanical transformation of rough diamonds into brilliant ones is usually achieved by polishing using microsized abrasive diamond particles. It is shown that in addition to formation of periodic pattern of 'partial' Hertzian cone cracks on the diamond surface, nano-sized domains (50-150 nm in diameter) of crumbled material are observed. Because these domains are located in the centres of the regions (250-500 nm in diameters) partially surrounded by the Hertzian cone cracks, where the stresses are close to the stress field of hydrostatic compression, the material removal cannot be explained by creation of tensile or shear cracks. It is argued that the creation of these domains of crumbled material is due to adhesive interactions between sliding diamond particles and the diamond surface. Employing a two-term law of friction, the scheme of ultimate equilibrium between the particle and the surface is presented. The distributions of contact stresses are calculated for two approaches: (i) the extended JKR (Johnson-Kendall-Roberts) model, and (ii) the 'soft' model of adhesive contact. Thus, adhesion between the sliding diamond particle and the surface leads to creation of periodic pattern of the crumbling domains with the steps 500-1000 nm and adhesive tearing out the material from the domains.

1. Introduction

Carbon has the symbol C and it is the 6th chemical element of the Mendeleev periodic table. Carbon-based materials are the age-old topic of research. For many years, these studies were concentrated on diamond, graphite and various coals. In 1797 S. Tennant showed experimentally that diamond is an allotrope of carbon. Now it is well-known that graphite is a carbon allotrope with sp^2 hybridization, while diamond is the allotrope with sp^3 carbon bond hybridization, i.e. the carbon atoms in diamond are bonded together in a tetrahedral lattice arrangement, while these atoms in graphite are bonded together in hexagonal lattices, which are then layered in parallel sheets connected by van der Waals bonds. The interest in the well-known carbon allotropes such as graphite and diamond is still very high. Indeed, diamond possesses a unique combination of outstanding physical and chemical properties, in particular, it has the highest hardness of all known materials. Due to their very specific electrical, mechanical, and tribological properties, diamonds and diamond coatings have many technical applications [20,57]. Because natural diamond is a very rare and expensive material, there were many attempts to increase the size of the diamonds or make synthetic diamonds [17]. Thus, P.W. Bridgman suggested to produce synthetic diamonds using high temperatures and pressure. As far back as in 1956, B.V. Derjaguin and his co-worker B.V. Spitsyn introduced the chemical vapour deposition (CVD) process and pioneered the study of the problem of diamond synthesis at reduced pressures [62]. In 1975, Derjaguin and Fedoseev published a paper [17] and then a book [18] where they described the results of Derjaguin's laboratory in the area of carbon-based materials and presented a review of previous efforts in production of synthetic diamonds.

Diamond is often referred to as the king of the gemstones. If these gemstones are faceted and polished then they are called brilliant diamonds and such jewels are very expensive. The polishing of diamond is very difficult due to its very high hardness and chemical inertness. There are several comprehensive reviews of literature related to techniques of polishing diamonds and modelling of the related processes [14,41].

To the best of our knowledge, Tolokowsky [65] presented the the first detailed study of polishing of diamonds. His results are discussed in details by Wilks and Wilks [66], and Hird and Field [41]. According to the Tolokowsky theory, the material removal during mechanical polishing of diamond is due to micro-cleavage process. However, this theory was later criticized [41,44]. The material removal mechanism were discussed by many authors. In addition to mechanical polishing, other mechanisms of material removal were discussed [13,41] including mechanisms caused by phase transformation, diamond oxidation and graphitization.

It is well-known that diamonds heated to a sufficiently high temperature may transform to graphite (see, e.g. [10,59]). Because diamonds are thermodynamically unstable, their graphitization may occur at the spots of high pressure. Indentation techniques are intensively used to study mechanical properties of both natural [12,50,62] and synthetic diamonds [21,36]. The estimations of the average contact pressure in a diamond sample under Vickers indenter is about 135 GPa and this stress may cause graphitization of the material [26]. This prediction was confirmed experimentally and pressure-induced phase transformations in diamond were observed [35]. The situation is similar to the situation related to sliding wear of other carbon-based materials (see, e.g. [3,6], namely wear mechanisms may vary depending on environmental atmosphere or temperature. Graphitization may occur due to the temperature rise at the points of interlocking of asperities, where effects of both high pressure and high flash temperature may combine. The strength of the material spots where the phase transition occurred is negligible [63]. Hence, it may be easily removed. Some observations of Bowden and Hanwell on diamond friction in vacuum [10], may get the same explanations as friction and wear of carbon-nitride coatings [3]: the protuberances of the diamond surface interlock with asperities of the counter-face surface. This causes the flash temperature rise and graphitization of the protuberances. The graphitized protuberances sheared away from the surface and the surface becomes very smooth. However,

friction may be high even for smooth surfaces due to presence of unsaturated dangling bonds along with effects caused by molecular adhesion.

Thus, although processes related to polishing diamond were studied by many authors [14,22], challenges remain for obtaining a satisfying understanding of the contributions of atomic and nano-scale effects to the processes accompanying removal of the material [13,41,66]. The recent papers [11,44] dedicated to studies of atomic mechanisms of diamond fracture and literature reviews on diamond polishing [13,41,66] show that this research area is still very actual and the studying of mechanisms of diamond polishing remains the topical problem.

Here the process of mechanical polishing of natural diamonds is discussed. It is described and explained a new mechanism of abrasive wear of diamond monocrystals that results in formation of nanocracks and adhesive craters of torn out material on the diamond surface. The results presented here are based on experimental and theoretical studies of mechanics of diamonds fulfilled in the former Soviet Union (see, e.g. [1,29,36,63]). Unfortunately, after the collapse of the country, there were various problems that did not allow the authors to continue their intensive studies of natural diamonds. Although the main results presented here were obtained by two authors (BG and OG) and presented in their preprint in 1994 [27], these results have never been published and developed further except the development of the Johnson-Kendall-Roberts (JKR) theory [47] (see discussions of the JKR formalism in [4,5,8,56]). We see that the models introduced by the authors and the mechanism of abrasive wear mentioned above [27] have not been rediscovered by other researchers.

During the above mentioned studies, an experiment was implemented when the temperature was varied in the friction zone between rotating scaife containing diamond powder and the diamond. The variation of the temperature was from relatively low (about 290 K) to high (more than 1500 K). It was found that depending on temperature, diamonds may behave as brittle elastic solids or as plastic ones. The temperature T_{br} of transition from brittle to plastic behaviour under local loading conditions is defined as the temperature of crack disappearance in hardness tests [37]. It was shown that T_{br} corresponds to the transition brittleness–plasticity temperature determined on micro-samples during standard tests [38]. For samples of natural diamond containing different amounts of nitrogen impurities, T_{br} varied in the range of 1420–1470 K, which is equal to about 70% of temperature of intensive graphitization, which plays the role of the melting temperature when calculating the mechanical properties of diamond [64] in the region of its metastability. Note that T_{br} approximately coincides with the temperature of the brittleness–plasticity transition, determined by the study of the temperature dependence of the ultimate strength of a diamond during bending [1]. Indeed, it was found that $T_{br} \approx 1470$ K according to indentation tests, while $T_{br} \approx 1500$ K according to bending tests. It was also found that with an increase of temperature up to 1000 K, the removal rate increased sharply, and then it fell to negligible rate with the further heating to 1500 K and above. Hence, for the temperature range of 1000–1400 K, it was observed the minimum values of the contact strength and, accordingly, it took place the maximization of the contact fracture of a diamond under quasi-static loading or during sliding of an abrasive grain. For this temperature interval, a core of plastic deformation under the contact region is formed. Hence, the fracture occurs as a result of a combined action of the contact stresses due to the elastic interaction between two bodies and the stresses due to this plastic core.

Thus, the studies of dependence of mechanical behaviour of diamonds on temperature showed: (i) elastic indentation of diamond particles into diamonds with creation of Hertzian cracks is observed at temperatures 290–1000 K; (ii) elastic-plastic indentation of diamond particles with creation of plastic imprints surrounded by radial and lateral cracks and for sliding particles, creation of chevron cracks with crumbling of material, is observed at temperatures 1000–1400 K; and (iii) transition to fully plastic regime of diamond deformations and almost complete absence of abrasive removal of the material is observed at temperatures 1500 K and above. Hence, the main part of the technological process of making of brilliant diamonds was at the temperature

interval 1000-1400 K, when the maximum of abrasive removal of material is observed, while the final stage of fine diamond polishing was at temperatures 290-1000 K.

Further we consider only the final stage of diamond mechanical polishing. At this stage, one may observe on the surface a periodic pattern of nano-sized regions surrounded by Hertzian cracks and domains where the materials has been torn-out due to adhesion. The domains are located at the centres of the regions. Employing a two-term law of friction, the scheme of ultimate equilibrium between the particle and the surface is presented. The adhesive interactions are described using two approaches: (i) the extended JKR (Johnson-Kendall-Roberts) model [47] having infinite tensile stresses at the edge of the contact zone, and (ii) a self-consistent theory of adhesion (the 'soft' model of adhesive contact) having bounded tensile stresses within the contact zone [42]. The latter model is described by two types of non-linear boundary integral equations, in displacements and in stresses respectively. These equations were studied using numerical approaches. On the other hand, for power-law shapes of diamond particles, one can derive quite simple analytical expressions with the framework of the JKR formalism. The distributions of contact stresses are calculated for each of the adhesive models. It is argued that the wear of diamond may be caused by adhesive interactions between abrasive diamond particles and diamond surface and the well-known formation of semi-circle Hertz-type nano-cracks is accompanying by creation of discrete nano-sized domains of the torn-out material.

2. A new mechanism of diamond removal during polishing

For experimental studies, we have used mono-crystals of natural diamonds that were cut and polished using diamond powders. The diameters of diamond particles were in the range 7 – 20 μm .

Mechanical diamond polishing was carried out by a rotating cast iron disc ('scaife') having diameter 300 mm. It was rotating with a speed of 3000 RPM and vertical beats 3-5 μm . The diamond powders were embedded in pre-machined ring grooves ('stripes').

(a) The abrasive patterns observed on the surface of polished diamond

Fig. 1 presents a microscopic image of a diamond surface at the final stage of polishing process. One can see partial circles of Hertzian cracks and the domains (craters) of torn-out material. To provide better visualization of the process, we have presented a schematic of the image.

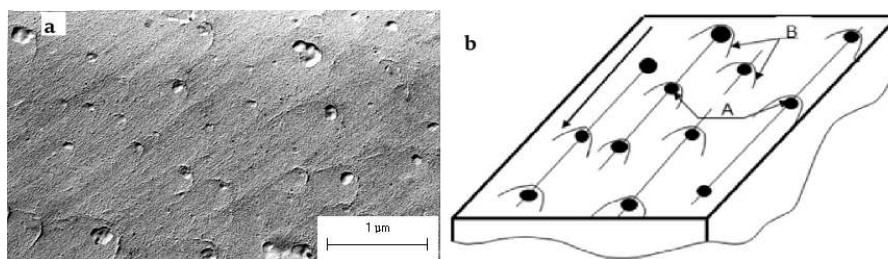


Figure 1. Traces of sliding diamond particles and fragmentation pattern on a polished diamond surface: (a) a microscopic image (at 32000 magnification) of partial circles of Hertzian cracks and the domains (craters) of torn-out material; (b) schematic of adhesive craters of torn-out material (A) and partial Hertzian cracks (B).

The pattern unit consists of a 'partial' Hertzian cone crack, whose size may vary in the range of 250 - 500 nm and a domain of 50-150 nm located in the center of the region surrounded by the Hertzian crack. The pattern units separated by steps of 500-1000 nm. It is assumed that material of the domains (craters) may be torn out due to adhesion with the sliding abrasive particle. It could also have a phase transition due to high hydrostatic compression within the domain. We point

out that the observed formation of adhesive breaks occurs under conditions of domination of the Hertz fracture, which, according to our experimental data, occurs up to temperatures of about 1000 K. The adhesive interactions and Hertzian fracture detected at temperatures below 1000 K and the processes of plastic deformation of the material, its combustion and graphitization at temperatures above 1500 K are of lesser importance for productivity during preparation of the brilliant diamonds, but the low temperature polishing can be used at the finishing stages of the process to ensure the desired quality in terms of the height of the surface irregularities.

(b) Fracture models of hard materials due to local high pressure.

As it was noted by Hertz, the contact loading of a spherical indenter may cause the cracking of solids. The questions related to fracture of materials due to contact between solids are discussed in many papers and books (see, e.g. [51,53]). Frank and Lawn developed the first theory of Hertzian fracture [23,54]. They studied the tensile stresses at the periphery of the circular contact region. It was assumed that the cracks may appear at the edge of the contact region, while as it was noted by Wilshaw [67], generally the Hertzian cracks initiate outside the contact region. One can note that the papers dedicated to Hertzian fracture and published over 50 years ago, discussed cracking just by calculation of stress fields in the contact problem and they did not consider the changes of the stress fields due to crack propagation. Fig. 2 shows mosaic, block structure of the diamond surface layers during cutting and grinding for (a): (100); (b): (111); and (c): (112) crystal planes. The surface structures can be related to nano-cracking and micro cleavage phenomena.

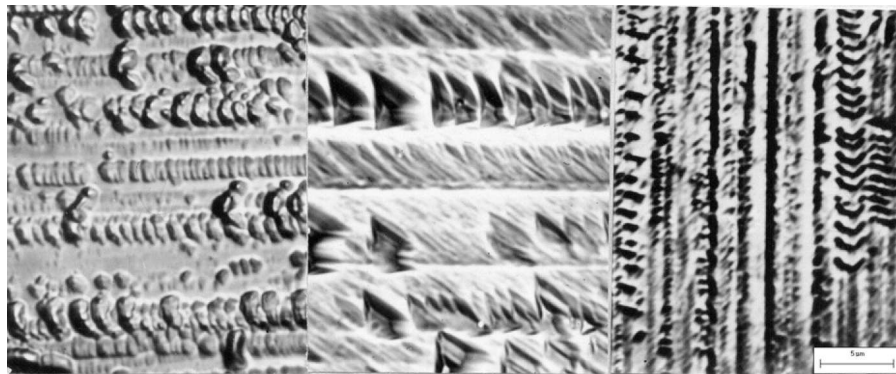


Figure 2. Surfaces of cutting and grinding diamond after etching. Block structure and fracture for (a): (100); (b):(111); and (c): (112) crystal planes. The surface structures can be related to nano-cracking and micro cleavage phenomena, formation of partial cone cracks and fragmentation patterns of diamond.

There are many papers and books dedicated to brittle fracture of materials due to indentation (see, e.g. [51,53]). Hertz [40] was the first researcher who mentioned creation of cracks due to punch indentation. Contact fracture of glass samples under action of a small spherical indenter demonstrates a rather sophisticated behaviour: median cracks and plastic deformation within a core region along with occasionally Hertzian cone cracks form during the loading cycle, while radial cracks and lateral cracks occur on the unloading cycle [53].

Problems of contact fracture were also studied for elastic-plastic materials. Analysing elastic-plastic indentation it was noted [46] that it is very difficult to calculate the contact stresses due to an elastic-plastic indentation in practice because the shape and size of the elastic-plastic boundary is not known *a priori*. Johnson suggested to describe the contact surface under the indenter being encased in a semi-spherical 'core' of radius a where a hydrostatic component of stress acts. The ideas of the Johnson core model were used and developed further by many authors (see, e.g. [28,30]). Because fracture of many hard brittle materials may result not only in creation

of system of isolated cracks but also in crushing of materials under the indenter or its phase transition. To describe contact fracture of such materials, it was introduced the so-called GG model of crushing of brittle porous materials [28], that was applied later to describe crushing of coals [52]. According to the GG model, there arise three regions of fracture: (i) the core of crushed material under the indenter, (ii) an intermediate region having radial crack fracture, and (iii) an elastic region surrounding other regions. However, the model will not be applied here because there is no evidence that the core of crushed (graphitic) material may be fully developed in diamond samples.

Our experimental studies show that almost circular Hertzian fracture may be observed in diamonds during indentation of both spheres and pyramids [26]. Indeed, the comparison of stress fields and displacements caused by pyramidal and spherical indenters shows that at a small distance from the contact region periphery, the fields are similar. However, due to anisotropy of diamonds, contact between a pyramid (either Vickers or Berkovich indenter) and a polished surface of a single crystals of orientation $\langle 001 \rangle$ leads to creation of a Hertzian crack having polygonal shape with sides oriented along $\langle 110 \rangle$. There were also observed lateral and near surface cracks. Other studies [36] showed that at ambient temperatures, plastic deformations in a single crystal of natural diamond are localized within a thin layer near the contact surface and the indentation has mainly elastic character. Hence, models of contact between elastic solids will be employed further.

3. Models of normal contact for diamond surfaces

Let us consider some specific features of problems of interactions between diamond surfaces loaded normally to their surfaces.

(a) Non-adhesive contact models

Diamond and other cubic crystals are comparatively isotropic [36]. Hence, we will employ contact models established for isotropic elastic solids.

The non-adhesive Hertz-type contact problem formulation assumes that initially there is only one point of contact between the body and the half-space. Let the origin (O) of Cartesian x_1, x_2, x_3 coordinates be at the point of initial contact between the body and the elastic half-space $x_3 \geq 0$. The cylindrical coordinate frame r, z, ϕ , $r = \sqrt{x^2 + y^2}$, $z = x_3$ and $x_1 = r \cos \phi$, $x_2 = r \sin \phi$. Hence, the equation of the body whose shape is given by a function f , can be written as $x_3 = -f(x_1, x_2)$, $f \geq 0$. We will consider further that the problem is axisymmetric, therefore it does not depend on the coordinate ϕ and we can write $z = -f(r)$.

It follows from the Hertz contact theory [33,46] that the problem of contact between a rigid body and an isotropic linear elastic half-space characterised by the Young's modulus E and the Poisson ratio ν depends on a contact modulus (reduced modulus) of the half-space E^*

$$E^* = \frac{E}{1 - \nu^2}. \quad (3.1)$$

The contact problem for two elastic solids having contact moduli E_1^* and E_2^* respectively is mathematically equivalent to the problem of contact between an isotropic elastic half-space with contact modulus E^*

$$\frac{1}{E^*} = \frac{1}{E_1^*} + \frac{1}{E_2^*} \quad (3.2)$$

and a curved body whose shape function f is equal to the initial distance between the surfaces, i.e. $f = f_1 + f_2$, where f_1 and f_2 are the shape functions of the solids. If the contact interactions cause the normal pressure $p(x_1, x_2)$ within the finite region of contact G then one obtains for the

problem of normal frictionless contact (see for details [33,46,55])

$$\delta - f(\mathbf{x}) = \frac{1}{\pi E^*} \iint_G K(\mathbf{x}, \mathbf{y}) p(y_1, y_2) dy_1 dy_2, \quad (3.3)$$

where K is the standard kernel

$$K(\mathbf{x}, \mathbf{y}) = \left((x_1 - y_1)^2 + (x_2 - y_2)^2 \right)^{-1/2}, \quad P = \iint_G p(y_1, y_2) dy_1 dy_2,$$

δ is the relative approach of the bodies, G is the contact region, $\mathbf{x} = (x_1, x_2)$, $\mathbf{y} = (y_1, y_2) \in G$, and P is the external load.

If one employs the isotropic elastic model of Hertz-type contact between two diamond surfaces, then

$$E^* = \frac{E}{2(1 - \nu^2)} = 583 \text{ GPa}. \quad (3.4)$$

It follows from the above discussion that in the problem of contact between two elastic spheres of radii R_1 and R_2 respectively, one gets the equivalent body as a sphere of radius R ,

$$(R)^{-1} = (R_1)^{-1} + (R_2)^{-1}. \quad (3.5)$$

The flat surface of the diamond crystal may be considered as a sphere of infinite radius, i.e. $R_2 = \infty$. Hence, and $R = R_1$, where R_1 is the particle radius.

The above discussion is related to contact between non-conforming surfaces. However, the shape of the abrasive particle may change due to wear and even undeformed surfaces may conform rather closely. The distances between undeformed conforming surfaces may be described as

$$f(r) = B_m r^m, \quad (3.6)$$

where $m > 2$ and B_m is a shape constant. Note that in the general case the shapes (3.6) include not only conforming surfaces but also non-conforming surfaces, e.g. a spherical body can be well approximated by monomial functions of degrees $m = 2$ and $B_2 = 1/(2R)$ and a cone is the case $m = 1$. Shtaerman [60,61] argued that the worn surfaces may be approximated by (3.6) with $m = 2n$ with $n > 1$. Galin considered the case of arbitrary real $m > 1$ [32,33]. Further the force and the approach for non-adhesive Hertz-type contact problem will be denoted by P_H and δ_H , respectively. Let us introduce functions $C(m)$ and $\chi(m)$

$$C(m) = \frac{m^2}{m+1} 2^{m-1} \frac{[\Gamma(m/2)]^2}{\Gamma(m)}, \quad \chi(m) = \frac{1}{m+1} \left\{ 4m^{m-1} \frac{\Gamma(m)}{[\Gamma(m/2)]^2} \right\}^{1/m}$$

where Γ is the Euler gamma function.

Then Galin's $P_H - \delta_H$ relations [32,33] may be written as

$$P_H = \left[\frac{(E^*)^m}{C(m)B_m} \right]^{\frac{1}{m+1}} \left(\frac{2m}{m+1} \right) \delta_H^{(m+1)/m} \quad (3.7)$$

and

$$P_H = B_m E^* \chi(m) (a/a')^{m+1}, \quad \delta_H = B_m (a/a')^m$$

where $a' = (m+1)\chi(m)/(2m)$.

(b) The JKR-type adhesive contact models

The above Hertz-type contact problems do not take adhesion into account between the diamond surface and a particle. To study problems of adhesive contact interactions, we need to specify the equilibrium distance between molecules as z_0 and to employ the concept of the work of adhesion w per a unit surface that is equal to the tensile force integrated through the distance necessary to pull the two surfaces completely apart [39] (see for details [4,55]). We can take the value of the work of adhesion for diamond as $w = 10 \text{ N/m}$.

There are various models of adhesive contact between solids. The adhesive contact problems have been studied mainly for elastic solids having spherical surfaces [49,55] and the most popular are the JKR (Johnson-Kendall-Roberts) [47] and DMT (Derjaguin-Muller-Toporov) [19] models. These models are discussed in detail elsewhere (see, e.g. [55]).

To decide which theory (the DMT or JKR) should be employed, one may use the Maugis parameter λ_M

$$\lambda_M = \frac{2}{0.97\pi} \sqrt[3]{\frac{4}{3} \frac{\delta_c}{z_0}} \approx 0.73 \frac{\delta_c}{z_0}, \quad \delta_c = \frac{3}{4} \left(\frac{\pi^2 w^2 R}{(E^*)^2} \right)^{1/3}. \quad (3.8)$$

Maugis [55] showed that if $\lambda_M > 5$ then the JKR theory may be used and if $\lambda_M < 0.1$ then one can employ the DMT theory. If one estimates z_0 as the distance between the cleavage planes of the diamond, i.e. $z_0 = 2 \cdot 10^{-10}$ m, and substitutes the above mentioned values R for diamond particles $3.5 - 10 \mu\text{m}$, then one gets λ_M is much greater than 5 and, therefore the JKR theory should be employed.

The historical development of the JKR theory was described by Kendall [49]. The Derjaguin balance energy approach [16] and the idea of superposition of stress field for the Hertz and Boussinesq contact problems [45] was used for solving problem of adhesive contact between two linearly elastic spheres [47].

The JKR formalism means that we solve an adhesive contact problem employing formally solutions to two non-adhesive contact problems (the Hertz-type and the Boussinesq-type problems) combining with the Derjaguin balance energy approach.

The JKR formalism may be used if the distance between the free surface of the material and the indenter surface increases rapidly at the periphery of the contact region and the solutions of two contact problems having the same contact area may be superimposed on each other [5].

Considering adhesive contact between spheres, Johnson wrote an expression for the work done in compression by the combined pressure (extracted from the Hertz and Boussinesq contact problems), and finally obtained an expression for the elastic strain energy stored in the two bodies (see (5.45) in [46]). However, it is difficult to get expressions for pressure under bodies having more general shape than spherical. There is a rather sophisticated expressions presented by Shtaerman [60,61]. Relatively recently expressions for both the elastic energy and complementary energy in the case of the axisymmetric adhesive indentation of an elastic half-space with an *a priori* unknown area of contact have been presented by Argatov and Mishuris [2], who attacked the problem within the framework of Griffith's criterion of equilibrium fracture. Borodich [4] also considered both the elastic energy and complementary energy to attack the problem of adhesive contact within the framework of the reinforced JKR formalism. As it has been mentioned above, here the stored elastic strain energy is presented in the same way as in the preprint [27], i.e. contrary to the expression through distributions of pressures by Johnson [46], here it is expressed through approaches h and h' . Using (3.7), one can write

$$U_E = aE^* \left(\frac{2m^2}{(m+1)(2m+1)} h^2 + \frac{2m}{m+1} h h' + h'^2 \right), \quad \delta = h + h' \quad (3.9)$$

where h' is the approach caused by adhesive attraction. One can write the expression for the total energy U_T as

$$U_T = U_E + U_S, \quad U_S = -w\pi a^2$$

where U_S is the surface energy, and employ the Griffith condition of system equilibrium

$$\partial U_T / \partial a = 0 = E^* h'^2 - 2\pi w a,$$

in order to obtain that $h' = -(2w\pi a / E^*)^{1/2}$.

This approach allowed us to write a numerical code for calculation of normal pressure within the contact region and obtain $P - \delta$ relations.

It was shown that the JKR formalism may be reinforced if one employs the properties of slopes of the force-displacement diagrams of non-adhesive indentation [4]. The reinforced JKR formalism may be applied to enormous number of adhesive contact problems for various elastic

structures [5,56]. In particular, it has been shown that in the JKR-type contact problems, the connections between the external force P , the approach of solids δ and the radius of the contact region can be written as

$$P = P_H - \sqrt{8\pi w E^* a^3}, \quad \delta = \delta_H - \left(\frac{2\pi w a}{E^*} \right)^{1/2}. \quad (3.10)$$

Using Galin's solution [32,33] for power-law shaped solids (3.6), one can represent (3.10) as

$$P = C(m) E^* B_m a^{m+1} - \sqrt{8\pi w E^* a^3}, \quad (3.11)$$

and

$$\delta = B_m C(m) \frac{m+1}{2m} a^m - \left(\frac{2\pi w a}{E^*} \right)^{1/2}. \quad (3.12)$$

It follows from (3.11) that the radius a of the contact region at $P = 0$ is

$$a(0) = \left[\frac{8\pi w}{E^* C^2(m) B_m^2} \right]^{1/(2m-1)},$$

while the force of adhesion P_c can be calculated by (3.11) at the contact radius

$$a = a_c = \left[\frac{9\pi w (a')^{2m}}{2m^2 B_m^2 E^*} \right]^{1/(2m-1)}.$$

As it is known, the choice of the characteristic parameters of the adhesive contact problem is rather arbitrary. For example, one can take as the characteristic radius $a_1^* = (m+1)\chi(m)/(2m)$ or another radius $a_2^* = a(0)$ can be used as a characteristic size of the contact region in order to write dimensionless parameters. Their connection can be written as

$$a(0) = \left\{ 8\pi w (a_1^*)^{2m+2} / [B_m^2 E^* \chi(m)^2] \right\}^{1/(2m-1)}.$$

If $\bar{p}(r')$ is the solution of the integral equation

$$\int_0^{2\pi} \int_0^{a_1^*} \frac{\bar{p}(\rho) \rho d\rho d\phi}{[(r')^2 + \rho^2 - 2r'\rho \cos \phi]^{1/2}} = 1 - (r')^m, \quad 0 \leq r' \leq a_1^*,$$

then the normal pressure can be written as

$$p(r') = \eta \{ \bar{p}(r') - \xi [(a_1^*)^2 - (r')^2]^{-1/2} \}, \quad r' = r(a_1^*/a)$$

where

$$\eta = \pi E^* B_m (a/a_1^*)^{m-1}, \quad \xi = (a_1^*/a)^m \left(\frac{2wa}{\pi^3 E^* B_m^2} \right)^{1/2}.$$

Using these above expressions, the normal stresses within the contact region have been calculated. The graphs of dimensionless pressures $p(r')/\eta$ for $a = a_c$ and for $m = 1, \dots, 5$ are shown in Fig. 3. It is known that even at the maximum of the tensile contact force, i.e. at $P = P_c$, the pressure p is negative within the central part of the contact region (see, Fig. 5.9 in [46]). However, the numerical simulations showed that even for $P = P_c$, the adhesive contact between conforming surfaces whose shapes are described by (3.6) with $m > 2.6$, the contact pressure is negative, i.e. there is no compression in the contact area.

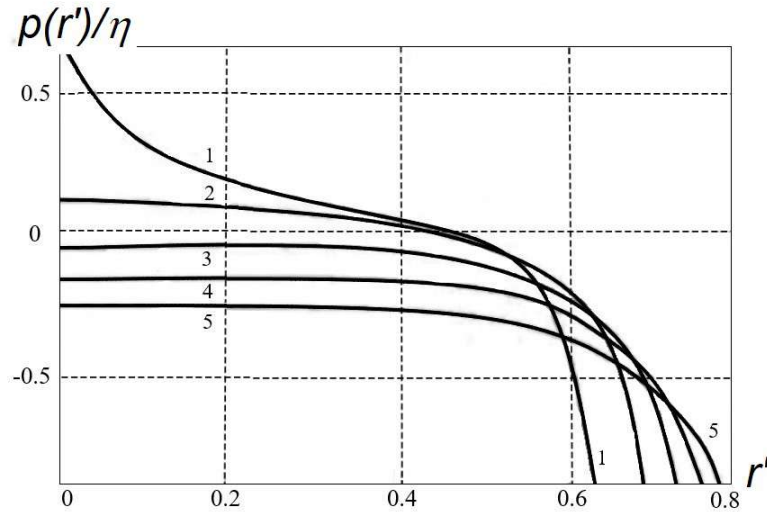


Figure 3. Dimensionless contact pressure in the framework of the extended JKR theory for $P = Pc$. The graph number is the same as the value of m .

Let us write the characteristic parameters of the adhesive contact problems as

$$a^* = a(0), \quad P^* = \left\{ \frac{(8\pi w)^{m+1} (E^*)^{m-2}}{[C(m)B_m]^3} \right\}^{\frac{1}{2m-1}}, \quad \delta^* = \left[\frac{2^{m+1}}{C(m)B_m} \left(\frac{\pi w}{E^*} \right)^m \right]^{\frac{1}{2m-1}}. \quad (3.13)$$

Then (3.11) and (3.12) have the following form

$$P/P^* = (a/a^*)^{m+1} - (a/a^*)^{3/2} \quad (3.14)$$

and

$$\frac{\delta}{\delta^*} = \frac{m+1}{m} \left(\frac{a}{a^*} \right)^m - \left(\frac{a}{a^*} \right)^{1/2}. \quad (3.15)$$

As it has been mentioned above, the shape of the gap between worn particle and the diamond surface may be described by (3.6). Hence, the dimensionless force-displacement curves of the JKR theory for worn particles may be obtained from (3.14) and (3.15). Fig. 4 shows these relations for $m = 2, \dots, 6$.

The pressure distribution of the Boussinesq problem for a flat-ended circular indenter goes to infinite at the periphery of the contact region. Because this solution is the fundamentally integral part of the JKR theory, the JKR solutions have always infinite stresses at the edge of the contact region.

4. The 'soft' model of adhesive contact

Discussing the Boussinesq-Kendall adhesive contact problem for a circular flat-ended indenter, Kendall [48] noted an analogy between the adherence of a flat punch and the fracture of a deeply notched bar. This comment inspired Maugis to employ the linear fracture mechanics method to

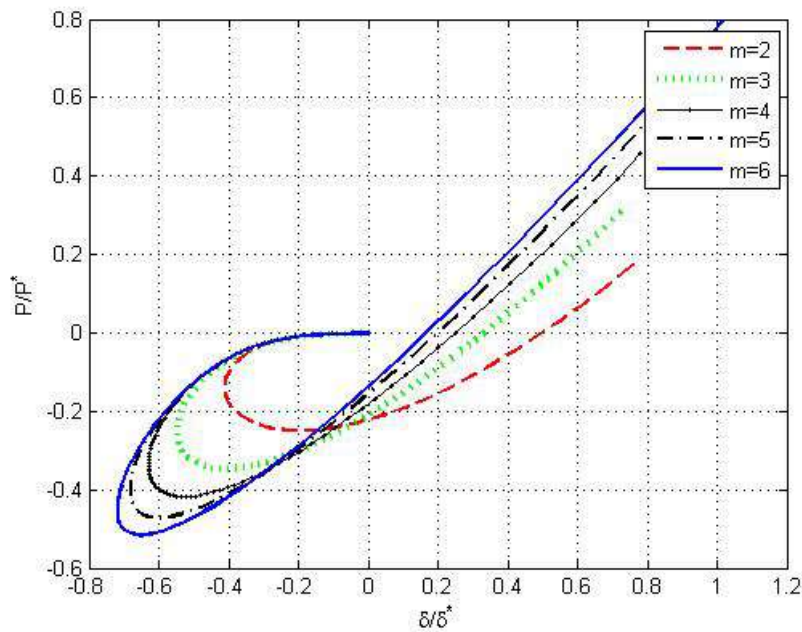


Figure 4. Dimensionless $P - \delta$ diagrams for power-law shaped indenters according to the JKR theory of adhesive contact.

adhesive contact (see e.g. [55]). Hence, one can reformulate the JKR theory of adhesive contact using the Griffith energy balance and the Irvin concept of the stress intensity factors. The ‘soft’ model of adhesive contact [42] may be considered as an application of the Barenblatt crack model to mechanics of adhesive contact. In the framework of ‘soft’ model, contrary to the JKR theory, there are no infinite stresses at the edge of the contact region. The tensile stresses cannot exceed the diamond tensile fracture stress σ_f . In general, one cannot obtain an analytic solution in the case of the ‘soft’ adhesive contact. Hence, an integral equations was derived that may be solved numerically.

To perform the numerical simulations, we apply the method of non-linear boundary integral equations (NBIE) developed for studying various unilateral contact problems, including problems for solids of complex shape and complicated boundary conditions on a contact surface [24,25]. The method was also discussed [7] in application to contact problems for non-convex indenters.

To formulate the problem, we will follow the chapter 5.5 of the classic Johnson book [46]. Let the force p per unit surface area (the pressure) be defined as (see Fig. 5.7 in [46])

$$p(z) = F(z)$$

where z is the separation between surfaces and F is a functional expression, e.g. the Lennard-Jones expression

$$F(z) = A_1 z^{-k} - A_2 z^{-n}, \quad k > n > 0, \quad A_1 > 0, \quad A_2 > 0. \tag{4.1}$$

At the equilibrium distance z_0 , we have $F(z_0) = 0$. Note that for practical application, the expression (4.1) should be truncated and it is assumed that $F(z) = 0$ for $z > z_m$, where z_m is some critical distance.

It is clear that atoms and molecules cannot penetrate each other. Effectively, this fact can be reflected by introducing some limit d_0 such that $F(z)$ is defined only for $d_0 \leq z$; it is described by

(4.1) for $d_0 < z$, and $F(d_0) = \infty$. This idea is very similar to idea of the hard sphere potential [43]. A similar idea was also discussed for modelling of deformations of nanoscale asperities [9,58], namely it was suggested to approximate the force, i.e. a derivative of the Lennard-Jones potential, as a bilinear expression: a linear Hooke's law for a spring for $d_0 \leq z$ (a derivative of the parabolic approximation of the potential at $z = z_0$) and an infinite force at $z = d_0$.

Let $\delta = (\delta_1, \delta_2, \delta_3)$ be an unknown vector of the approach δ_1 and unknown angles of rotation of the indenter as a rigid body δ_2 and δ_3 . Let M_{x_1} , M_{x_2} be the given external moments and P be the given vertical external load. Then one can write the NBIEs that replaces formulation of the contact problem for pressure p

$$p(\mathbf{x}) = F \left\{ \left[g(\mathbf{x}) + (\pi E^*)^{-1} \iint_G K(\mathbf{x}, \mathbf{y}) p(\mathbf{y}) d\mathbf{y} \right]^+ + d_0 \right\}, \quad \mathbf{x}, \mathbf{y} \in G \quad (4.2)$$

$$\iint_G p(\mathbf{x}) d\mathbf{x} = P, \quad \iint_G x_2 p(\mathbf{x}) d\mathbf{x} = M_{x_1}, \quad \iint_G x_1 p(\mathbf{x}) d\mathbf{x} = M_{x_2}$$

where $g(\mathbf{x}) = z_m - d_0 + f(\mathbf{x}) - \delta_1 - \delta_2 x_1 - \delta_3 x_2$.

To solve the Hertz-type contact problem in displacements, we consider not a traditional formulation of the contact problem, but rather the following NBIE with an unknown function $v(\mathbf{x})$

$$v(\mathbf{x}) = \left\{ g(\mathbf{x}) + (\pi E^*)^{-1} \iint_G K(\mathbf{x}, \mathbf{y}) F[v^+(\mathbf{y}) + d_0] d\mathbf{y} \right\}^+, \quad \mathbf{x}, \mathbf{y} \in G. \quad (4.3)$$

$$\iint_G F[v^+(\mathbf{x}) + d_0] d\mathbf{x} = P, \quad \iint_G x_2 F[v^+(\mathbf{x}) + d_0] d\mathbf{x} = M_{x_1}, \quad \iint_G x_1 F[v^+(\mathbf{x}) + d_0] d\mathbf{x} = M_{x_2}.$$

where the upper index $+$ denotes the positive part of the function, e.g. v^+ is defined as

$$v^+(\mathbf{x}) = \sup\{v(\mathbf{x}), 0\}.$$

Solving (4.2), we obtain the pressure p within the contact region, and solving (4.3), we obtain the function v and the vector of displacements.

5. Models of adhesion of sliding diamond particles

Let us model the process of adhesive wear of a natural diamond crystal during contact interaction with diamond sliding particles. It was argued that in a model of adhesive contacts under cyclic loading conditions, stress singularities may be induced by adhesive forces [34]. Here we present an alternative contact model. We argue that in the state of ultimate equilibrium between the sliding particle and the substrate, the contact region may become multiple-connected, in turn this leads to creation of very high tensile stresses that formally may exceed the tensile strength of diamond σ_f .

Fig. 5 presents a schematic of Hertzian 'partial' cone crack formation and a domain of torn-out material (adhesive crater) under a sliding diamond particle loaded by the external normal P and shear T forces. The shear force T is equal to the force of friction.

It is known (see discussions in [9,31]) that Amontons presented verbal formulation of three laws of friction in 1699. Two correct laws may be written as (i) the polishing force experienced by two dry bodies is independent of the dimensions of the bodies; and (ii) the polishing force is proportional to the applied normal force. In 1774 Kotelnikov introduced the notion of coefficient of friction μ and wrote the Amontons laws as a formula $T = \mu P$. In 1778 Coulomb proposed a two-term formula $T = A + \mu P$ where A is a parameter that depends on adhesive force between two bodies. The two term expression for the force of friction was not popular and it was forgotten for a long while. Often the classic one-term Amontons-Kotelnikov law is attributed to Coulomb.

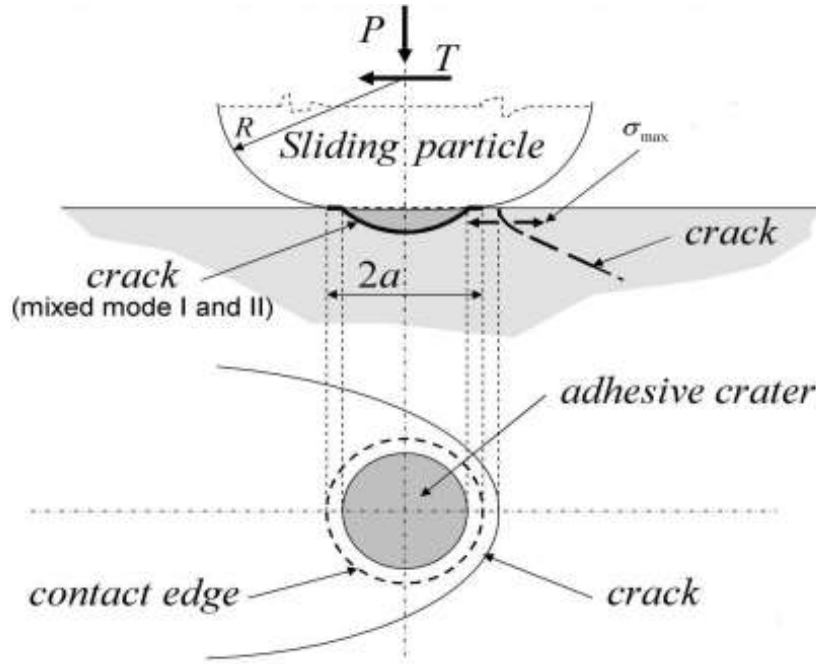


Figure 5. Schematic illustrating crack formation under a sliding diamond particle loaded by the external normal P and shear T forces.

Independently of Coulomb, Derjaguin [15] introduced a two-term law of friction and gave physical meaning and connected the law to adhesion. Following to Derjaguin, one can write

$$T = \mu(P + |P_c|) \quad (5.1)$$

where P_c is the critical force of adhesion of a spherical particle of radius R according to the JKR theory, i.e.

$$P_c = -(3/2)\pi wR.$$

To explain the above choice for the shear force, let us consider a schematic of the particle and acting forces in the state of ultimate equilibrium (see Fig. 6). The force T has an arm R , hence the overturning moment of forces is equal to TR . The region of contact between the surface and the particle at the state of ultimate equilibrium may be not a simply connected one and it may be subdivided into two separate contact subregions with centres: A and B . As one can see in Fig. 6), the arm h of the resultant normal force may be calculated as

$$h = \frac{TR}{P + |P_c|} = \frac{T\mu(P + |P_c|)R}{P + |P_c|} = \mu R. \quad (5.2)$$

Assuming the distributions of the tensile stresses within these two subregions can be estimated by employing the above described models of adhesion (Model 1 is the JKR-type model and Model 2 is the 'soft' model of adhesive contact), the pressures were calculated. Note that the normal stresses in a real material cannot exceed the tensile strength of diamond σ_f . As it has been mentioned, for worn particles having conforming surfaces (3.6) with $m > 2.6$ and $P = P_c$, the contact pressure is negative, i.e. there is no compression in the contact area.

Let us explain the model using a simple example of spherical particle of radius R , i.e. $m = 2$. In this case, the results of the classic JKR model may be used. As one can see in the neighbourhood of point A in Fig. 6), there is a region of compressive pressure of radius $a_c/\sqrt{3}$ where a_c is the radius of the whole contact subregion A . Due to its motion, the particle is transformed into non-equilibrium state when the fracture starts to be developed. Initially, the fracture arises at the

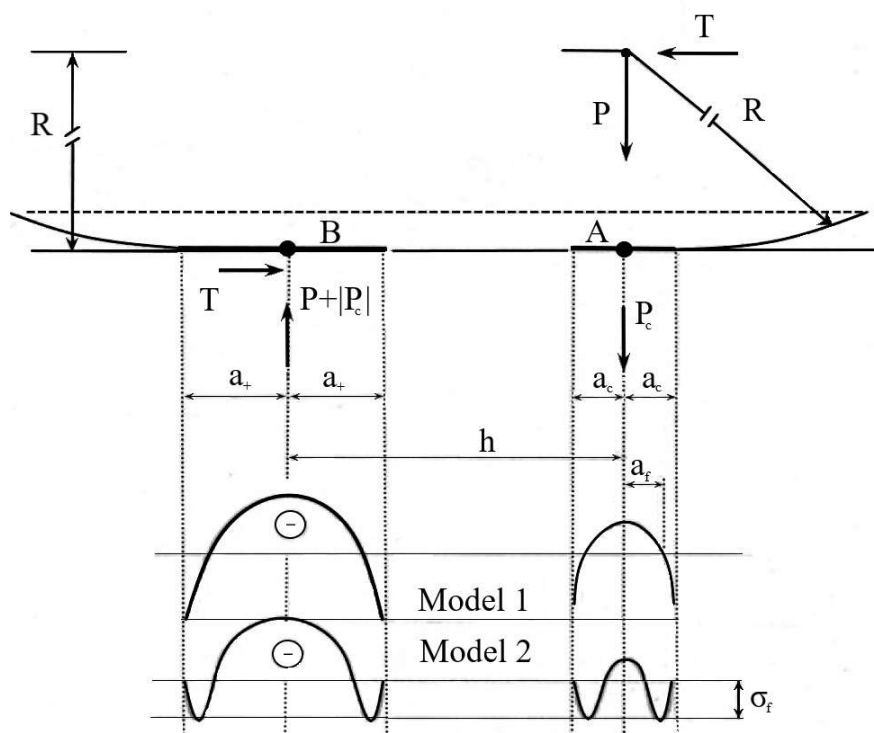


Figure 6. Schematics illustrating of force moments and two schemes of adhesive contacts and the corresponding stress field exhibiting tensile JKR singularity (Model 1) and the self-consistent contact stress field with non-singular stress concentration at the edge of the contact area (Model 2).

periphery of the contact subregion *A* where the tensile stresses are high, then it goes along the surface separating the particle-substrate pair and bends from this surface in order to envelop the semi-spherical core of the compressive stresses of radius $a_f = a_c/\sqrt{3}$. As a result, the material of this region is torn out creating adhesive craters observed in experiments. After the fracture was fully developed and the material of the domain was torn out, the particle is transferred in a new state of ultimate equilibrium, when the subregion *B* becomes a new contact subregion *A* and the size of the subregion reduces from a_+ to a_c . In this process, the arm of the moment h given by (5.2), defines the steps between the adhesive craters (the domains of crumbled material).

If the coefficient of friction μ for the diamond-diamond pair slipping along the soft directions, is $\mu = 0.1$ then it follows from (5.2) for particles of radii $3.5 - 10 \mu\text{m}$, that the steps are 350-1000 nm that pretty well agrees with experimental observations. The theoretically predicted sizes of the adhesive craters $a_f = a_c/\sqrt{3}$ that are 90-180 nm are also in good agreement with experimentally observed (50-150 nm).

6. Conclusion

Mechanical transformation of rough diamonds into brilliant ones is usually achieved by polishing using abrasive diamond particles whose characteristic radii are about 5-10 micrometres. A new mechanism of abrasive wear of diamond monocrystals is described and explained. It has been shown that in addition to formation of periodic pattern of 'partial' Hertzian cone cracks on the diamond surface, there are observed nano-sized domains (50-150 nm in diameter) of crumbled material that was torn out from the surface. Because these domains are located in the centres of

the regions (250-500 nm in diameters) partially surrounded by the Hertzian cone cracks, where the stresses are close to the stress field of hydrostatic compression, the material crumbling cannot be explained by creation of tensile or shear cracks. The mechanism described occurs at temperatures below 1000 K. It is argued that the creation of these domains of crumbled material is due to adhesive interactions between sliding diamond particles and the diamond surface.

To model the stress field in the contact regions, we have discussed two kinds of models of adhesive contact: (i) the extended JKR (Johnson-Kendall-Roberts) model that may be applied not only to spherical particles, but also to particles having conforming surfaces; (ii) self-consistent model ('soft' model) of adhesion. Numerical simulations showed that the overturning moment of forces acting on the particle may cause tensile stresses that nominally exceed the tensile strength of diamond, and, in turn they may cause that material may be torn out.

Thus, adhesive interactions between abrasive diamond particles and diamond surface cause formation of semi-circle Hertz-type nanocracks and discrete areas of crashing material lead to wear of diamond. The comparison of the theoretically predicted sizes of adhesive craters (the domains of torn-out material) and the steps between these discrete distributed craters are in good agreement with experimentally observed dimensions.

Authors' Contributions. BG and OG: initial idea of the study, FB, BG and OG: literature review (Section 1), FB and BG: developed the JKR formalism (Section 4), OG: experimental studies; BG: theoretical models and numerical simulations; FB: drafting of the manuscript. All authors read and approved the manuscript.

Competing Interests. The authors declare that they have no competing interests.

Acknowledgements. The authors are grateful to Professor K. Kendall, FRS for his interest in the topic of the research and his invitation to publish the materials of our studies.

References

1. Apteckman AA, Bakun OV, Grigor'ev ON, Trefilov VI 1986 Deformation and fracture of diamond in bending tests in the temperature range 300-2100 K. *Soviet Physics Doklady*, **31**, 839.
2. Argatov I, Mishuris G 2018 *Indentation testing of biological materials*. Springer.
3. Borodich FM 2013 Physical and Chemical Processes Affecting Performance of Super-low Friction Carbon Nitride Coatings in Various Gaseous Environments. In: Proc. of the 5th World Tribology Congress 2013 (WTC 2013), Torino, Italy.
4. Borodich FM 2014 The Hertz-type and adhesive contact problems for depth-sensing indentation. *Advances in Applied Mechanics*, **47**, 225–366.
5. Borodich FM 2022 The JKR formalism in applications to problems of adhesive contact. Ch 12. In: *Contact Problems for Soft, Biological and Bioinspired Materials*, Eds. Borodich F.M. and Jin X., Springer. ISBN 978-3-030-85174-3
6. Borodich FM, Chung Y-W, Keer LM (2008) Environmental and surface chemical effects on tribological properties of carbon-based coatings. In: *Tribology of Diamond-Like Carbon Films*, Eds. Donnet, C. and Erdemir, A., Springer, 282-290.
7. Borodich FM, Galanov BA (2002) Self-similar problems of elastic contact for non-convex punches. *J. Mech. Phys. Solids*, **50**, 2441-2461.
8. Borodich FM, Galanov BA, Suarez-Alvarez MM 2014 The JKR-type adhesive contact problems for power-law shaped axisymmetric punches. *J. Mech. Phys. Solids*, **68**, 14–32.
9. Borodich FM, Savencu O (2017) Hierarchical models of engineering rough surfaces and bio-inspired adhesives. Ch. 10 in: *Bio-inspired adhesives*. Eds. L. Heepe, S. Gorb and L. Xue, Springer, 179–219.
10. Bowden FP, Hanwell AE 1966 The friction of clean crystal surfaces. *Proc. R. Soc. Lond. A*, **295**, 233-243.
11. Brenner DW, Shenderova OA (2015) Theory and modelling of diamond fracture from an atomic perspective. *Phil. Trans. R. Soc. A*, **373**, 201401
12. Chaudhri MM 2020 Indentation hardness of diamond single crystals, nanopolycrystal, and nanotwinned diamonds: A critical review. *Diamond Related Materials*, **109**, 108076.
13. Chen Y, Zhang LC (2009) On the polishing techniques of diamond and diamond composites. *Key Engineering Materials*, **404**, 85-96.
14. Chen Y, Zhang L (2013) *Polishing of Diamond Materials*. London, Springer-Verlag.

15. Derjaguin B (1934a) Molekulartheorie der äußeren Reibung. *Zeitschrift Physik*, **88**, 661–164.
16. Derjaguin B (1934b) Untersuchungen über die Reibung und Adhäsion, IV. Theorie des Anhaftens kleiner Teilchen. *Kolloid Zeitschrift*, **69**, 155–164.
17. Derjaguin BV, Fedoseev DV (1975) The synthesis of diamond at low pressure. *Sci. Am.*, **233**, 102–109.
18. Derjaguin BV, Fedoseev DV (1977) Growth of Diamond and Graphite from the Gas Phase. Moscow, Nauka (in Russian).
19. Derjaguin BV, Muller VM, Toporov YP 1975 Effect of contact deformations on adhesion of particles. *J. Colloid Interface Sci.*, **53**, 314–326.
20. Donnet C, Erdemir A (Eds) (2008) Tribology of Diamond-Like Carbon Films, A., Springer.
21. Drory MD, Dauskardt RH, Kant A, Ritchie RO (1995) Fracture of synthetic diamond. *J. Appl. Phys.*, **78**, 3063–3068.
22. Field JE (Ed.) (1992) The Properties of Natural and Synthetic Diamonds, London: Academic Press.
23. Frank FC, Lawn BR (1967) On the theory of Hertzian fracture. *Proc. R. Soc. Lond. A*, **299**, 291–306.
24. Galanov BA (1985) The method of boundary equations of the Hammerstein-type for contact problems of the theory of elasticity when the regions of contact are not known. *J. Appl. Math. and Mech. PMM*, **49**, 634–640.
25. Galanov BA (1997) Nonlinear boundary integral equations of contact mechanics and some their engineering applications. In: L. Morino and W.L. Wendland (eds.), IABEM Symposium on Boundary Integral Methods for Nonlinear Problems, Kluwer Acad. Publ., 69–74.
26. Galanov BA, Grigoriev ON (1986) Deformation and fracture of superhard materials in concentrated loading. *Strength of Materials*, **18**, 1330–1337.
27. Galanov BA, Grigoriev ON (1994) Adhesion and wear of diamond. Part I. Modelling. Part 2. Experiments. Preprint. Institute for Problems in Materials Science., Nat. Ac. Sci. Ukraine, Kiev.
28. Galanov BA, Grigoriev ON (2006) Analytical model of indentation of brittle materials. In: "Electron Microscopy and Materials Strength", Eds.: S.A. Firstov et al. *Proceedings of Institute of Materials Science, Vol. 13*, Kiev, 4–42. (Russian)
29. Galanov BA, Grigor'ev ON, Milman YV, Ragozin IP (1983) Determination of the hardness and Young's modulus from the depth of penetration of a pyramidal indenter. *Strength of Materials*, **15**, 1624–1628.
30. Galanov BA, Milman YuV, Ivakhnenko SA, Suprun OM, Chugunova SI, Golubenko AA, Tkach VN, Litvin PM, Voskoboinik IV (2016) Improved inclusion core model and its application for measuring the hardness of diamond. *J. Superhard Mater.*, **38**, 289–305.
31. Galanov BA, Valeeva IK (2016) Sliding adhesive contact of elastic solids with stochastic roughness. *Int. J. Engineering Sciences*, **101**, 64–80.
32. Galin LA 1946 Spatial contact problems of the theory of elasticity for punches of circular shape in planar projection. *PMM J. Appl. Math. Mech.*, **10**, 425–448. (Russian)
33. Galin LA 1961 *Contact Problems in the Theory of Elasticity*, Ed. I.N. Sneddon, North Carolina State College, Departments of Mathematics and Engineering Research, NSF Grant No. G16447, 1961.
34. Giannakopoulos AE, Venkatesh TA, Lindley TC, Suresh S (1999) The role of adhesion in contact fatigue. *Acta materialia*, **47**, 4653–4664.
35. Gogotsi YG, Kailer A, Nickel KG, (1998) Pressure-induced phase transformations in diamond. *Journal of Applied Physics*, **84**, 1299–1304.
36. Grigor'ev ON (1982) Investigation of the plasticity and strength properties of superhard materials by microindentation methods. *Soviet Powder Metallurgy and Metal Ceramics*, **21**, 65–73.
37. Grigoriev O.N., Gridneva I.V., Milman Yu.I., Chugunova S.I., 1976 Fracture of diamond under local loading. In: *Physics of Brittle Fracture*, Kiev, Publishing house of IPM of the Academy of Sciences of the Ukrainian SSR, Part 1, 30–34.
38. Grigoriev O.N., Milman Yu.I., Trefilov V.I. 1976 Determination of the temperature of transition brittleness-plasticity for brittle materials based on the results of microindentation. In: *Physics of Brittle Fracture*, Kiev, Publishing house of IPM of the Academy of Sciences of the Ukrainian SSR, Part 1, 12–16.
39. Harkins WD 1919 Cohesion, internal pressure, adhesion, tensile strength, tensile energy, negative surface energy, and molecular attraction. *Proc. Natl. Acad. Sci. USA*, **5**, 562–568.
40. Hertz H 1882 Ueber die Berührung fester elastischer Körper. *J. reine angewandte Mathematik.*

- 92, 156–171. (English transl. Hertz H 1896 On the contact of elastic solids. In: *Miscellaneous Papers by H. Hertz*. Eds. D.E. Jones and G.A. Schott, Macmillan, London, 146–162).
41. Hird JR, Field JE (2004) Diamond polishing. *Proc. R. Soc. Lond. A*, **460**, 3547–3568.
 42. Hughes BD, White LR (1979) ‘Soft’ contact problems in linear elasticity. *Q. J. Mech Appl. Math.*, **32**, 445–471.
 43. Israelachvili JN (1991) *Intermolecular and Surface Forces*. Academic Press, London.
 44. Jarvis MR, Pérez R, Van Bouwelen FM, Payne MC (1998) Microscopic mechanism for mechanical polishing of diamond (110) surfaces. *Physical Review Letters*, **80**, 3428.
 45. Johnson KL (1958) A note on the adhesion of elastic solids. *Brit. J. Appl. Phys.*, **9**, 199–200.
 46. Johnson KL (1985) *Contact Mechanics*. Cambridge University Press, Cambridge.
 47. Johnson KL, Kendall K, Roberts AD (1971) Surface energy and the contact of elastic solids. *Proc. R. Soc. Lond. A*, **324**, 301–313.
 48. Kendall K (1973) An adhesion paradox. *The Journal of Adhesion*, **5**, 77–79. DOI: 10.1080/00218467308078440
 49. Kendall K 2001 *Molecular Adhesion and Its Applications*. Kluwer Academic/Plenum Publishers, New York.
 50. Khrushchov MM, Berkovich ES (1951) Methods of determining the hardness of very hard materials: the hardness of diamond. *Industrial Diamond Review*, **11**, 42–49.
 51. Kolesnikov YuV, Morozov EM (1989) *Mechanics of Contact Fracture*. Nauka, Moscow. (Russian)
 52. Kossovich EL, Borodich FM, Epshtein SA, Galanov BA (2020) Indentation of bituminous coals: fracture, crushing and dust formation. *Mechanics of Materials*, **150**, 103570. doi:10.1016/j.mechmat.2020.103570
 53. Lawn BR (1993) *Fracture of Brittle Solids*. Cambridge University Press, Cambridge.
 54. Lawn BR (1967) Partial cone crack formation in brittle material loaded with a sliding spherical indenter. *Proc. R. Soc. Lond. A*, **299**, 307–316.
 55. Maugis D (2000) *Contact, Adhesion and Rupture of Elastic Solids*. Springer-Verlag, Berlin.
 56. Perepelkin NV, Borodich FM (2021) Explicit transition between solutions to non-adhesive and adhesive contact problems by means of the classical Johnson-Kendall-Roberts formalism. *Phil. Trans. R. Soc. A*, **379**, 20200374. (doi.org/10.1098/rsta.2020.0374)
 57. Piotrowski PL, Cannara RJ, Gao G, Urban JJ, Carpick RW, Harrison JA (2010) Atomistic factors governing adhesion between diamond, amorphous carbon and model diamond nanocomposite surfaces. *J. Adhesion Science and Technology*, **24**, 2471–2498.
 58. Savencu O (2016) Simulations of dry friction between rough surfaces and corresponding nonlinear problems at nano and microscales. PhD thesis, Cardiff University
 59. Seal M 1958 Graphitization and plastic deformation of diamond. *Nature*, **182**, 1264–1267.
 60. Shtaerman IYa 1939 On the Hertz theory of local deformations resulting from the pressure of elastic solids. *Dokl. Akad. Nauk SSSR*, **25**, 360–362 (Russian).
 61. Shtaerman IYa (Steuermann EJ) 1949 *Contact Problem of Elasticity Theory* Gostekhizdat, Moscow (Russian)
 62. Spitsyn BV, Deryagin BV 1956 A Technique of Diamond Face Regrowth. Authors certificate SU 339134, Files 964957/716358.
 63. Trefilov VI, Borisenko VI, Grigor’ev ON, Mil’man YuV (1975) Temperature dependence of the hardness and the plastic deformation mechanism for diamond. *Soviet Physics Doklady*, **19**, 464–467.
 64. Trefilov VI., Milman Yu.V., Grigoriev O.N. 1988 Deformation and rupture of crystals with covalent interatomic bonds. *Progress in Crystal Growth and Characterization*, **16**, 225–277.
 65. Tolkowsky M 1920 Research on the abrading, grinding or polishing of diamond. DSc thesis (Eng.), City and Guilds College, University of London
 66. Wilks EM, Wilks J (1972) The resistance of diamond to abrasion. *J. Phys. D: Appl. Phys.*, **5**, 1902–1919.
 67. Wilshaw TR 1971 The Hertzian fracture test. *J. Phys. D: Appl. Phys.*, **4**, 1567–1581.